Galvanic Replacement of Semiconductor Phase I CuTCNQ Microrods with KAuBr 4 to Fabricate CuTCNQ/Au Nanocomposites with Photocatalytic Properties

ARTICLE · JANUARY 2011

CITATIONS
7

READS
30

4 AUTHORS:

Andrew Pearson
RMIT University
20 PUBLICATIONS **270** CITATIONS
SEE PROFILE

Anthony Peter O'Mullane
Queensland University of Technology
149 PUBLICATIONS **1,918** CITATIONS
SEE PROFILE

Vipul Bansal
RMIT University
150 PUBLICATIONS **3,204** CITATIONS
SEE PROFILE

Suresh Bhargava
RMIT University
431 PUBLICATIONS **3,703** CITATIONS
SEE PROFILE

Inorganic Chemistry
Article

Inorg. Chem. **2011**, *50*, 1705–1712 **1705**
DOI: 10.1021/ic1021752

Galvanic Replacement of Semiconductor Phase I CuTCNQ Microrods with $KAuBr_4$ to Fabricate CuTCNQ/Au Nanocomposites with Photocatalytic Properties

Andrew Pearson, Anthony P. O'Mullane,* Vipul Bansal,* and Suresh K. Bhargava*

School of Applied Sciences, RMIT University, GPO Box 2476 V, Melbourne, Australia

Received October 28, 2010

In this study, the reaction of semiconductor microrods of phase I copper 7,7,8,8-tetracyanoquinodimethane (CuTCNQ) with $KAuBr_4$ in acetonitrile is reported. It was found that the reaction is redox in nature and proceeds via a galvanic replacement mechanism in which the surface of CuTCNQ is replaced with metallic gold nanoparticles. Given the slight solubility of CuTCNQ in acetonitrile, two competing reactions, namely CuTCNQ dissolution and the redox reaction with $KAuBr_4$, were found to operate in parallel. An increase in the surface coverage of CuTCNQ microrods with gold nanoparticles occurred with an increased $KAuBr_4$ concentration in acetonitrile, which also inhibited CuTCNQ dissolution. The reaction progress with time was monitored using UV−visible, FT-IR, and Raman spectroscopy as well as XRD and EDX analysis, and SEM imaging. The CuTCNQ/Au nanocomposites were investigated for their photocatalytic properties, wherein the destruction of Congo red, an organic dye, by simulated solar light was found dependent on the surface coverage of gold nanoparticles on the CuTCNQ microrods. This method of decorating CuTCNQ may open the possibility of modifying this and other metal-TCNQ charge transfer complexes with a host of other metals which may have significant applications.

1. Introduction

Metal−organic semiconducting materials based on charge transfer complexes of metal-7,7,8,8-tetracyanoquinodimethane (TCNQ) have received considerable attention over the past 40 years, with a particular resurgence in interest in the past few years through the work of Dunbar et al., Miller et al., and Bond et al.[1−19] In particular, CuTCNQ has been the subject of intensive research given the observation of a switching effect from a high to low impedance state upon the application of an electric field or optical excitation.[20−25] It has also been demonstrated that CuTCNQ can exist in two phases, namely, phase I that has a room temperature conductivity of 0.2 S cm^{-1} and phase II with a conductivity of 10^{-5} S cm^{-1}. There have been many attempts to synthesize

*To whom correspondence should be addressed. E-mail: vipul.bansal@rmit.edu.au (V.B.); anthony.omullane@rmit.edu.au (A.P.O.); suresh.bhargava@rmit.edu.au (S.K.B.).

(1) Heintz, R. A.; Zhao, H.; Ouyang, X.; Grandinetti, G.; Cowen, J.; Dunbar, K. R. *Inorg. Chem.* **1999**, *38*, 144–156.
(2) Zhao, H.; Heintz, R. A.; Ouyang, X.; Grandinetti, G.; Cowen, J.; Dunbar, K. R. *NATO ASI Ser., Ser. C: Math. Phys. Sci.* **1999**, *518*, 353–376.
(3) O'Kane, S. A.; Clerac, R.; Zhao, H.; Ouyang, X.; Galan-Mascaros, J. R.; Heintz, R.; Dunbar, K. R. *J. Solid State Chem.* **2000**, *152*, 159–173.
(4) Miyasaka, H.; Motokawa, N.; Matsunaga, S.; Yamashita, M.; Sugimoto, K.; Mori, T.; Toyota, N.; Dunbar, K. R. *J. Am. Chem. Soc.* **2010**, *132*, 1532–1544.
(5) Clerac, R.; O'Kane, S.; Cowen, J.; Ouyang, X.; Heintz, R.; Zhao, H.; Bazile, M. J., Jr.; Dunbar, K. R. *Chem. Mater.* **2003**, *15*, 1840–1850.
(6) Wang, X.; Liable-Sands, L. M.; Manson, J. L.; Rheingold, A. L.; Miller, J. S. *Chem. Commun.* **1996**, 1979–1980.
(7) Vickers, E. B.; Selby, T. D.; Thorum, M. S.; Taliaferro, M. L.; Miller, J. S. *Inorg. Chem.* **2004**, *43*, 6414–6420.
(8) Vickers, E. B.; Giles, I. D.; Miller, J. S. *Chem. Mater.* **2005**, *17*, 1667–1672.
(9) Garcia-Yoldi, I.; Miller, J. S.; Novoa, J. J. *J. Phys. Chem. A* **2009**, *113*, 7124–7132.
(10) Neufeld, A. K.; Madsen, I.; Bond, A. M.; Hogan, C. F. *Chem. Mater.* **2003**, *15*, 3573–3585.
(11) Neufeld, A. K.; O'Mullane, A. P.; Bond, A. M. *J. Am. Chem. Soc.* **2005**, *127*, 13846–13853.
(12) Harris, A. R.; Neufeld, A. K.; O'Mullane, A. P.; Bond, A. M. *J. Mater. Chem.* **2006**, *16*, 4397–4406.
(13) O'Mullane, A. P.; Neufeld, A. K.; Harris, A. R.; Bond, A. M. *Langmuir* **2006**, *22*, 10499–10505.
(14) Harris, A. R.; Nafady, A.; O'Mullane, A. P.; Bond, A. M. *Chem. Mater.* **2007**, *19*, 5499–5509.
(15) Nafady, A.; Bond, A. M.; Bilyk, A.; Harris, A. R.; Bhatt, A. I.; O'Mullane, A. P.; De Marco, R. *J. Am. Chem. Soc.* **2007**, *129*, 2369–2382.
(16) O'Mullane, A. P.; Fay, N.; Nafady, A.; Bond, A. M. *J. Am. Chem. Soc.* **2007**, *129*, 2066–2073.
(17) Nafady, A.; Bond, A. M. *Inorg. Chem.* **2007**, *46*, 4128–4137.
(18) Zhao, C.; MacFarlane, D. R.; Bond, A. M. *J. Am. Chem. Soc.* **2009**, *131*, 16195–16205.
(19) Nafady, A.; Bond, A. M.; O'Mullane, A. P. *Inorg. Chem.* **2009**, *48*, 9258–9270.
(20) Potember, R. S.; Poehler, T. O.; Benson, R. C. *Appl. Phys. Lett.* **1982**, *41*, 548–50.
(21) Xiao, K.; Ivanov, I. N.; Puretzky, A. A.; Liu, Z.; Geohegan, D. B. *Adv. Mater.* **2006**, *18*, 2184–2188.
(22) Muller, R.; Genoe, J.; Heremans, P. *Appl. Phys. Lett.* **2006**, *88*, 242105.
(23) Muller, R.; De Jonge, S.; Myny, K.; Wouters, D. J.; Genoe, J.; Heremans, P. *Solid-State Electron.* **2006**, *50*, 602–606.
(24) Oyamada, T.; Tanaka, H.; Matsushige, K.; Sasabe, H.; Adachi, C. *Appl. Phys. Lett.* **2003**, *83*, 1252–1254.
(25) Liu, H.; Liu, Z.; Qian, X.; Guo, Y.; Cui, S.; Sun, L.; Song, Y.; Li, Y.; Zhu, D. *Cryst. Growth Des.* **2009**, *10*, 237–243.

Published on Web 01/19/2011

CuTCNQ in various morphologies using chemical, electrochemical, and photochemical techniques; however, to date there has been little or no attempt to modify the surface of CuTCNQ once it has been formed.[26] Moreover, the application of CuTCNQ has been almost exclusively limited to switching and field emission devices.[20−30] However, in many instances, the modification of semiconducting materials with metallic nanoparticles achieved by physical, chemical, or electrochemical methods can open up the use of these semiconductor/metal composites to a wide variety of areas such as catalysis and sensing. For example, it is well documented that metal oxides such as TiO_2, SnO_2, and ZnO, which are utilized as supports for metal nanoparticles, are extremely effective photocatalysts for the removal of organic pollutants.[31−33]

A relatively recently explored area for the surface modification of films and solution-based nanomaterials is an elegant galvanic replacement process, in which two main approaches have thus been explored. In the first approach, sacrificial metal templates such as Ag, Co, Ni, and Cu are replaced with noble metals such as Au, Pd, and Pt to fabricate bimetallic colloids and surfaces. This has led to a variety of colloidal materials that can be hollow, highly porous, or dendritic in nature and nanostructured surfaces that show significant porosity or are decorated with spherical nanoparticles, continuous films, or dendrites.[34−43] The second approach is the replacement of Si surfaces with metals ions such as Au, Pd, Pt, Cu, and Ni. This approach is carried out in the presence of fluoride ions, which generally employs highly corrosive hydrofluoric acid (HF), to facilitate the formation of SiF_6^{2-}, thus alleviating any formation of SiO_2 that would inhibit the reaction.[44] In general, the oxidation of Si to SiF_6^{2-} is accompanied by a charge transfer through Si that allows metal deposition to occur at a different site on the surface, which is usually favored at defect sites.[44] It is also found that there can be significant roughening of the semiconducting surface using such an approach. In all cases, the thermodynamic driving force for the reaction is provided by the lower standard potential of the sacrificial metal/metal ion couple in comparison with that of the solution-based metal/metal ion couple.

However, to the best of our knowledge, the second approach has hitherto been limited to the traditional semiconducting materials used in the microelectronics industry such as Si, Ge, and GaAs. Moreover, this approach typically requires the use of corrosive HF to achieve galvanic replacement on semiconducting materials. In the current study, we have utilized the galvanic replacement approach for the first time to decorate semiconductor phase I CuTCNQ microrods with Au nanoparticles without involving HF during the process, wherein we have demonstrated that the surface coverage of CuTCNQ microrods with Au nanoparticles can be feasibly fine-tuned by controlling the gold salt concentration in the solution. It is also demonstrated that the phase I CuTCNQ/Au composite shows significant activity toward the photocatalytic degradation of organic dyes such as Congo red, which may open up the possibility of using this type of material for many other photocatalytic applications.

2. Methodology

Materials. Copper metal foil (99% purity) was obtained from Chem Supply. 7,7,8,8-Tetracyanoquinodimethane (TCNQ) was obtained from Fluka. Potassium tetrabromoaurate ($KAuBr_4 \cdot 3H_2O$), Congo red, and 4-nitrophenol were obtained from Sigma-Aldrich, and acetonitrile was obtained from BDH Chemicals. Copper foil was treated with dilute nitric acid, rinsed with water, and dried with a flow of nitrogen immediately prior to use. All other chemicals were used as received without modification.

Phase I CuTCNQ Synthesis. A $12 \times 1.5 \times 0.05$ cm^3 strip of copper foil was first immersed in dilute nitric acid to facilitate the removal of any oxide species on the copper surface. The copper foil was then washed with deionized water and immediately placed in 50 mL of a 5 mM TCNQ solution in acetonitrile. The surface of the copper foil was observed to turn black in color with a dark bluish/purplish tinge, indicating the formation of CuTCNQ, and the reaction was allowed to proceed for 1 h. The CuTCNQ foil was then washed three times with deionized water and dried under nitrogen. After the CuTCNQ foil was sufficiently washed and dried, the 12×1.5 cm^2 piece of foil was cut into eight 1.5×1.5 cm^2 pieces to ensure that all subsequent experiments were performed on the same batch of CuTCNQ.

Galvanic Replacement of CuTCNQ with $KAuBr_4$. Six 1.5×1.5 cm^2 pieces of CuTCNQ were each added to separate solutions containing increasing concentrations (1 μM, 10 μM, 50 μM, 100 μM, 500 μM, and 1 mM) of $KAuBr_4$ in 5 mL of acetonitrile. The galvanic replacement reaction between CuTCNQ and $KAuBr_4$ was then allowed to proceed for 4 h. After 4 h, the pieces of CuTCNQ were removed from solution and washed three times with deionized water to remove any residual $KAuBr_4$ or dissolved CuTCNQ. The solutions obtained after the galvanic replacement reaction were later analyzed by UV−visible spectroscopy (Cary 50 Bio spectrophotometer). The galvanically replaced CuTCNQ substrates were examined without any further modification using scanning electron microscopy (FEI NovaSEM), electron dispersive X-rays (EDX performed on an FEI NovaSEM instrument coupled with an EDX Si(Li) X-ray detector), X-ray photoelectron spectroscopy (Thermo K-Alpha XPS instrument at a pressure better than 1×10^{-9} Torr with core levels aligned with

(26) Liu, H.; Cui, S.; Guo, Y.; Li, Y.; Huang, C.; Zuo, Z.; Yin, X.; Song, Y.; Zhu, D. *J. Mater. Chem.* **2009**, *19*, 1031–1036.
(27) Duan, H.; Cowan, D. O.; Kruger, J. *Mater. Res. Soc. Symp. Proc.* **1990**, *173*, 165–169.
(28) Liu, S.-G.; Liu, Y.-Q.; Wu, P.-J.; Zhu, D.-B. *Chem. Mater.* **1996**, *8*, 2779–2787.
(29) Liu, H.; Zhao, Q.; Li, Y.; Liu, Y.; Lu, F.; Zhuang, J.; Wang, S.; Jiang, L.; Zhu, D.; Yu, D.; Chi, L. *J. Am. Chem. Soc.* **2005**, *127*, 1120–1121.
(30) Liu, Y. L.; Ji, Z. Y.; Tang, Q. X.; Jiang, L.; Li, H. X.; He, M.; Hu, W. P.; Zhang, D. Q.; Wang, X. K.; Wang, C.; Liu, Y. Q.; Zhu, D. B. *Adv. Mater.* **2005**, *17*, 2953–2957.
(31) Sharma, S. D.; Saini, K. K.; Kant, C.; Sharma, C. P.; Jain, S. C. *Appl. Catal., B* **2008**, *84*, 233–240.
(32) Mahmoodi, N. M.; Arami, M.; Limaee, N. Y.; Gharanjig, K. *J. Haz. Mater.* **2007**, *145*, 65–71.
(33) Barraud, E.; Bosc, F.; Edwards, D.; Keller, N.; Keller, V. *J. Catal.* **2005**, *235*, 318–326.
(34) Pearson, A.; O'Mullane, A. P.; Bansal, V.; Bhargava, S. K. *Chem. Commun.* **2010**, *46*, 731–733.
(35) O'Mullane, A. P.; Ippolito, S. J.; Bond, A. M.; Bhargava, S. K. *Electrochem. Commun.* **2010**, *12*, 611–615.
(36) Bansal, V.; O'Mullane, A. P.; Bhargava, S. K. *Electrochem. Commun.* **2009**, *11*, 1639–1642.
(37) Lee, C.-L.; Tseng, C.-M. *J. Phys. Chem. C* **2008**, *112*, 13342–13345.
(38) Guo, S.; Dong, S.; Wang, E. *Chem.—Eur. J.* **2008**, *14*, 4689–4695.
(39) Chen, Q.-S.; Sun, S.-G.; Zhou, Z.-Y.; Chen, Y.-X.; Deng, S.-B. *Phys. Chem. Chem. Phys.* **2008**, *10*, 3645–3654.
(40) Bansal, V.; Jani, H.; Du Plessis, J.; Coloe, P. J.; Bhargava, S. K. *Adv. Mater.* **2008**, *20*, 717–723.
(41) Au, L.; Lu, X.; Xia, Y. *Adv. Mater.* **2008**, *20*, 2517–2522.
(42) Lu, X.; Tuan, H.-Y.; Chen, J.; Li, Z.-Y.; Korgel, B. A.; Xia, Y. *J. Am. Chem. Soc.* **2007**, *129*, 1733–1742.
(43) Chen, J.; Wiley, B.; McLellan, J.; Xiong, Y.; Li, Z. Y.; Xia, Y. *Nano Lett.* **2005**, *5*, 2058–2062.
(44) Huang, Z.; Geyer, N.; Werner, P.; de Boor, J.; Gosele, U. *Adv. Mater.* **2011**, *23*, 285−308.

a C 1s binding energy of 285 eV), X-ray diffraction (XRD; Bruker AXS D8 Discover with General Area Detector Diffraction System), Fourier transform infrared spectroscopy (FT-IR Perkin-Elmer Spectrum 100), and Raman spectroscopy (Perkin-Elmer Raman Station 200F). In a control experiment, pristine CuTCNQ microrods grown onto copper foil were immersed in acetonitrile for 4 h to follow its spontaneous dissolution in acetonitrile. In another control experiment, to observe the effect of copper foil on the galvanic replacement reaction, CuTCNQ crystals grown onto copper foil were separated by scratching the surface, followed by the galvanic replacement of 1 mg of CuTCNQ powders (in the absence of Cu foil) with increasing concentrations (1 μM, 10 μM, 50 μM, 100 μM, 500 μM, 1 mM, and 10 mM) of $KAuBr_4$ in 5 mL of acetonitrile for 4 h.

Photocatalytic Experiments. The photocatalytic activity of the galvanically replaced phase I CuTCNQ substrates was examined by immersing a 1.5 × 1.5 cm^2 piece of CuTCNQ in a 5 mL, 50 μM aqueous solution of the organic dye, "Congo red" (CR), and recording the intensity of the characteristic absorption maxima at ca. 500 nm after exposure to simulated solar light (based on equator conditions) for a period of 30 min. An Abet Technologies LS-150 Series 150W Xe Arc lamp source with a condensing lens was used with the sample placed in a quartz vial at a distance of 7 cm from the source with slow mechanical stirring to promote mixing of the solution. After 30 min of irradiation, the composite was removed by centrifugation, and the remaining solution was examined by UV−vis spectroscopy. Additionally, the degradation of Congo red dye as a function of photoreaction time was monitored by total organic carbon (TOC) measurements for the CuTCNQ/Au sample prepared by reacting with 1 mM $KAuBr_4$. The TOC measurements were performed using a Sievers instrument.

3. Results and Discussion

The formation of phase I CuTCNQ through the spontaneous electrolysis technique has been well documented in previous studies.[30,45] Illustrated in Figure 1a are phase I CuTCNQ microrods that have been formed through the reaction of copper foil with an acetonitrile solution containing 5 mM TCNQ. It can be clearly seen that a dense coverage of CuTCNQ microrods that grow outward from the surface has been achieved. The rods have an average square cross-section of 1 × 1 μm with faceted corners and are 10−20 μm in length. Lower magnification SEM images are shown in the Supporting Information (Figure S1-a1), which demonstrate a uniform distribution of CuTCNQ microrods on the copper foil surface. The C, N, O, and Cu signals arising from these microrods in EDX analysis suggest that the observed structures are CuTCNQ crystals (Supporting Information, Figure S2, curve a). FT-IR spectroscopy analysis further confirms that the microrods are composed of phase I CuTCNQ, with characteristic vibration modes at 2199, 2171, and 825 cm^{-1} (Supporting Information, Figure S3, curve a).[1]

The reaction of phase I CuTCNQ with $KAuBr_4$ was then undertaken in an acetonitrile solution containing different concentrations of the gold salt. However, given that CuTCNQ is slightly soluble in acetonitrile to an estimated concentration of 0.14 mM,[46] the Cu foil with CuTCNQ microrods grown on both sides was first immersed in acetonitrile for 4 h to follow its dissolution. It can be seen in Figure 1b and Figure S1-b1 (Supporting Information) that

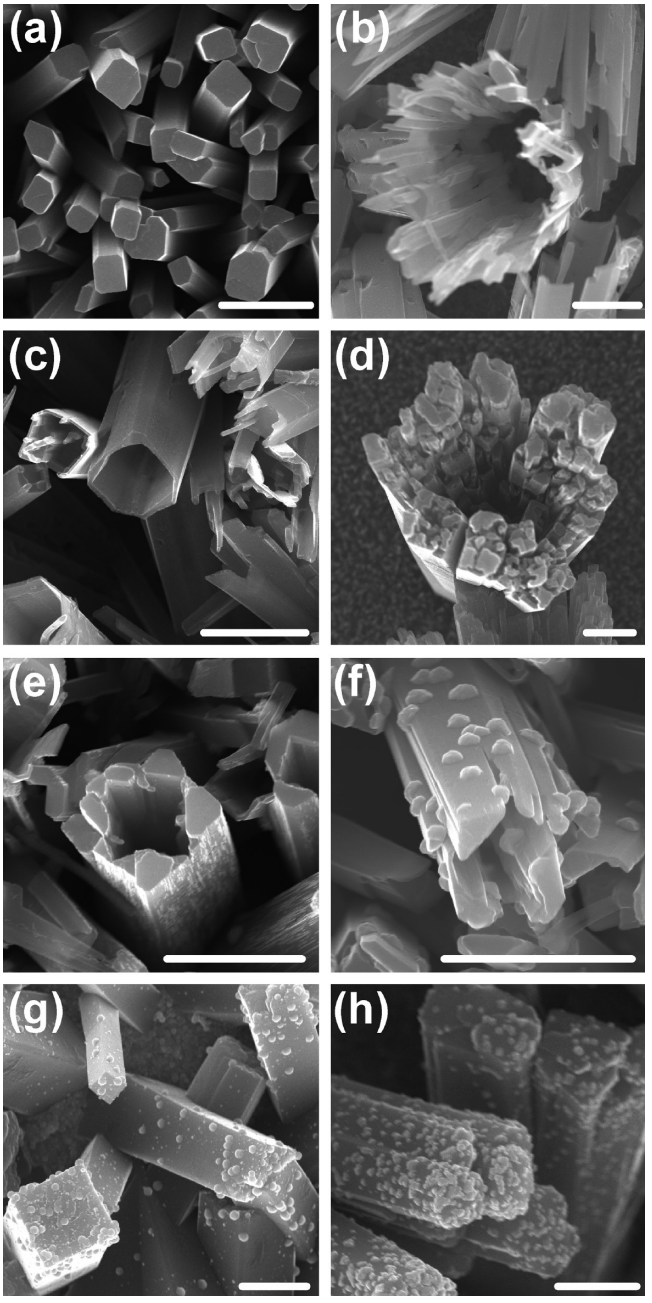

Figure 1. Scanning electron microscopy (SEM) images of (a) pristine CuTCNQ microrods; (b) CuTCNQ microrods immersed in acetonitrile for 4 h; and CuTCNQ microrods reacted with (c) 1 μM, (d) 10 μM, (e) 50 μM, (f) 100 μM, (g) 500 μM, and (h) 1 mM $KAuBr_4$ in acetonitrile. Scale bars correspond to 2 μm.

the CuTCNQ microrods dissolve in acetonitrile to leave behind a mixture of hollow microtubes with a wall thickness of ca. 50 nm and vertically oriented long plate-like structures that result from dissolution of three out of four long edges of the microrods. Interestingly, during CuTCNQ dissolution in acetonitrile, the length of the CuTCNQ microrods was not observed to change significantly. This type of effect has been observed by Liu and co-workers, who monitored CuTCNQ formation over time using the spontaneous electrolysis method. It was found that the dissolution rate eventually exceeds the formation rate, resulting in the formation of hollow CuTCNQ tubes.[45] Here, the only process occurring is the dissolution process, which is analogous to pitting corrosion

(45) Liu, Y.; Li, H.; Ji, Z.; Kashimura, Y.; Tang, Q.; Furukawa, K.; Torimitsu, K.; Hu, W.; Zhu, D. *Micron* **2007**, *38*, 536–542.
(46) Harris, A. R.; Neufeld, A. K.; O'Mullane, A. P.; Bond, A. M.; Morrison, R. J. S. *J. Electrochem. Soc.* **2005**, *152*, C577–C583.

and results in the rapid formation of CuTCNQ microtubes. Upon the addition of 1 μM $KAuBr_4$ in acetonitrile, the CuTCNQ microrods undergo a similar morphology change to that observed when no $KAuBr_4$ is present, whereby well-defined hollow CuTCNQ rods are observed with smooth, thin walls of ca. 50 nm in thickness (Figure 1c). Increasing the concentration of $KAuBr_4$ to 10 μM also results in etching of the CuTCNQ rods to form a pseudo-hollow structure; however, the degree of CuTCNQ dissolution into acetonitrile is observed to be significantly less than that observed for the lower concentration (1 μM) of $KAuBr_4$, as it can be seen that the etching has only partly dissolved the interior of the CuTCNQ rod (Figure 1d). The addition of 50 μM $KAuBr_4$ shows similar dissolution of CuTCNQ by acetonitrile compared to that observed for both 1 μM and 10 μM $KAuBr_4$ additions. However, the exterior walls of the CuTCNQ rods appear to undergo a transformation whereby the surface has become roughened by the deposition of sub-100-nm quasi-spherical nanoparticles (Figure 1e). These particles were confirmed to be Au by EDX analysis (Figure S2, Supporting Information) and can be more clearly seen in a side view image shown in the Supporting Information (Figure S1-e2). It is also of note that the dissolution of CuTCNQ has occurred primarily in the center of the CuTCNQ microrods at a square offset at ca. 90° to the microrods themselves.

Increasing the $KAuBr_4$ concentration to 100 μM results in the deposition of large 100−200 nm quasi-spherical Au particles with an increased density on the surface of the etched CuTCNQ microrods, where the etching has been significant enough to split the rod into four prongs, where the four corners of the CuTCNQ rod had once been connected (Figure 1f and Figure S1-f1, Supporting Information). Interestingly, further increasing the $KAuBr_4$ concentration to 500 μM during the reaction inhibits the etching process, thereby resulting in only minor etching at the top of the CuTCNQ rods while the surface appears roughened with the deposition of both large (100−200 nm) and small (sub-100 nm) quasi-spherical gold particles (Figure 1g). This effect becomes more pronounced when the $KAuBr_4$ concentration is further increased to 1 mM, which results in a significant increase in the number of Au nanoparticles decorating the surface of the CuTCNQ microrods, while little to no dissolution of CuTCNQ is observed (Figure 1h). At the highest $KAuBr_4$ concentration, the decoration with Au nanoparticles begins at the top of the CuTCNQ rods where almost complete coverage is observed and becomes sparser further down the CuTCNQ rod to the substrate surface.

The formation of Au nanoparticles on the surface of CuTCNQ during the reaction was also established by EDX analysis, which shows a continuous increase in the signature for Au upon increasing the gold salt concentration used during the reaction (Supporting Information, Figure S2). The FT-IR spectral analysis showed only the presence of phase I CuTCNQ under all conditions, illustrating that phase I CuTCNQ is not converted to phase II CuTCNQ during the galvanic replacement reaction (Supporting Information, Figure S3). The nature of the CuTCNQ/Au nanocomposite after reaction between phase I pristine CuTCNQ crystals and highest $KAuBr_4$ concentration used in this study (1 mM) was further verified using X-ray photoelectron spectroscopy

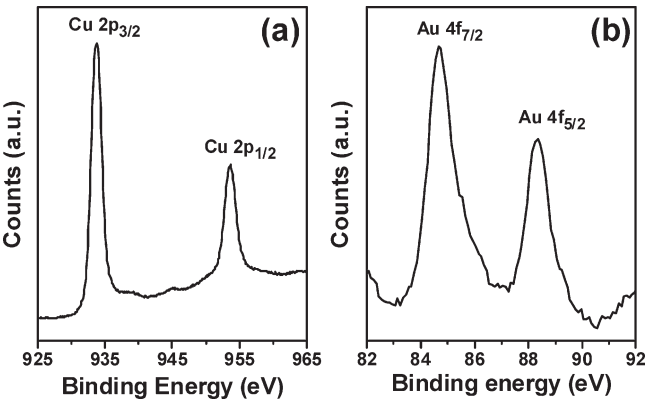

Figure 2. XPS analysis showing the (a) Cu 2p and (b) Au 4f core levels from CuTCNQ/Au nanocomposite obtained after the reaction of CuTCNQ crystals with 1 mM $KAuBr_4$ in acetonitrile.

(XPS), which is a highly surface sensitive technique and can provide crucial information about chemical species present in the system.[47] XPS analysis for Cu 2p and Au 4f core levels of the CuTCNQ/Au nanocomposite shown in Figure 1h is exhibited in Figure 2. The Cu 2p core level (Figure 2a) showed two characteristic $2p_{3/2}$ and $2p_{1/2}$ splitting components with sharp peaks arising at binding energies (BEs) of ca. 933.8 and 953.7 eV, respectively, which correspond to phase I CuTCNQ.[30] Additionally, no significant signature corresponding to shakeup satellites due to Cu^{2+} was observed, suggesting that the products remain predominantly Cu^{+} even after galvanic replacement with the highest concentration of Au^{3+} ions.[30] Moreover, XPS measurements also confirmed that the product formed after galvanic replacement essentially remains as phase I CuTCNQ without any signatures of CuBr formation, because in CuBr, the Cu $2p_{3/2}$ component is expected at 932.4 eV,[48] which is 1.4 eV lower than that observed in our system. Similar to Cu 2p, the Au 4f core level could be split into $4f_{7/2}$ and $4f_{5/2}$ components with a major $4f_{7/2}$ BE feature at ca. 84.7 eV, which is a characteristic of Au^0,[49] thus further confirming the formation of Au nanoparticles during the galvanic replacement reaction.

Given the substantial dissolution of CuTCNQ that seems to occur during the reaction with lower concentrations of $KAuBr_4$, the reaction solutions were monitored with UV−visible spectroscopy (Figure 3). Initially, a UV−vis spectrum of a solution in which a CuTCNQ substrate was immersed in acetonitrile for 4 h was recorded (brown curve). It is evident that a spectrum typical of $TCNQ^{-}$ ions in solution is recorded where several characteristic peaks above a wavelength of 600 nm are observed with a major peak at ca. 745 nm, a secondary peak at ca. 765 nm, and a shoulder at ca. 725 nm. Additional features over the 400−450 nm wavelength range can also be seen, which are indicative of $TCNQ^{-}$ ions.[50] This indicates that CuTCNQ dissolves to form $TCNQ^{-}$ and Cu^{+} ions in acetonitrile, where the latter species is assumed due to the high stability of Cu^{+} in this solvent.[46] As a reference, a UV−vis spectrum of 5 mM TCNQ in acetonitrile was also collected (orange dotted curve), which shows a typical strong absorption band centered at 390 nm and no evidence of spectral features above 650 nm, thus corroborating well with previous observations.[16,50]

(47) Bansal, V.; Syed, A.; Bhargava, S. K.; Ahmad, A.; Sastry, M. *Langmuir* **2007**, *23*, 4993–4998.

(48) Yang, M.; Zhu, J.-J.; Li, J.-J. *J. Crys. Growth* **2004**, *267*, 283–287.

(49) Joshi, H.; Shirude, P. S.; Bansal, V.; Ganesh, K. N.; Sastry, M. *J. Phys. Chem. B* **2004**, *108*, 11535–11540.

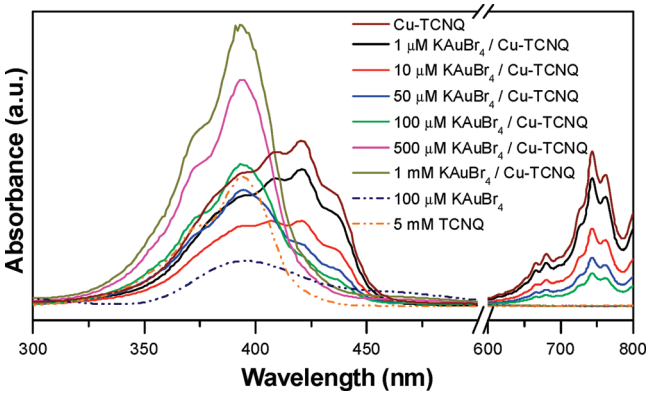

Figure 3. UV−visible spectra of solutions obtained after galvanic replacement of CuTCNQ with increasing concentrations of $KAuBr_4$ in acetonitrile.

UV−visible spectral analysis of the solutions in which CuTCNQ samples were reacted with increasing concentrations of $KAuBr_4$ indicates that the intensities of all of the features associated with $TCNQ^-$ above 650 nm decrease in proportion to the amount of $KAuBr_4$ added to the reaction, thus indicating a decrease in the amount of $TCNQ^-$ dissolving into acetonitrile. Significantly, upon the addition of 500 μM and 1 mM $KAuBr_4$, the intensity of the peaks attributable to $TCNQ^-$ falls to zero, which indicates that at higher gold salt concentrations, either little or no $TCNQ^-$ is dissolved into the solution. This observation is consistent with the SEM images, which show little to no etching of the CuTCNQ microrods at higher gold salt concentrations (Figure 1g and h). Similarly, in the 400−450 nm wavelength range, peaks attributable to $TCNQ^-$ are also observed to decrease, whereas a feature at 390 nm is observed to increase in intensity with increasing gold salt concentration. This is interesting, as it suggests the possibility of neutral TCNQ formation during the reaction of phase I CuTCNQ with $KAuBr_4$, which is highly soluble in acetonitrile. This feature at 390 nm becomes increasingly prominent with increasing gold salt concentration. The possibility of residual TCNQ from the CuTCNQ synthesis procedure may play a slight role but would not account for the increasing intensity of the band at 390 nm with increasing $KAuBr_4$ concentration. There may also be a contribution from unreacted $KAuBr_4$, whose spectrum is also shown (blue dotted curve); however, this is quite a broad feature (350 to 450 nm) and is not as sharp as the band associated with neutral TCNQ. This provides a strong argument in favor of the formation of a neutral TCNQ species during the reaction between CuTCNQ microrods and $KAuBr_4$ and suggests a galvanic replacement process does occur.

The observation of Au nanoparticles on the surface of CuTCNQ rods (Figure 1e−h) and a UV−vis spectral feature associated with neutral TCNQ suggests that a redox reaction occurs between phase I CuTCNQ and $KAuBr_4$ via the simultaneous reduction of Au^{3+} from $KAuBr_4$ and the oxidation of $TCNQ^-$ from CuTCNQ, whose rate is dependent on the concentration of $KAuBr_4$ used. A powerful method used to probe differences between TCNQ and materials containing $TCNQ^-$ anion radicals is Raman spectroscopy. Illustrated in Figure 4 are Raman spectra of solid films of

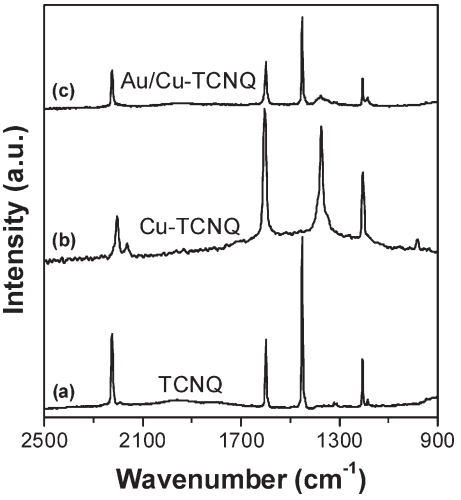

Figure 4. Raman spectra of (a) TCNQ crystals drop cast onto a polished gold substrate, (b) unmodified CuTCNQ substrate, and (c) CuTCNQ reacted with 1 mM $KAuBr_4$.

pristine TCNQ crystals (spectrum a), pristine phase I CuTCNQ (spectrum b), and CuTCNQ after being reacted with 1 mM $KAuBr_4$ (spectrum c). Pristine TCNQ crystals exhibit four characteristic principle vibration modes at ca. 1200 cm^{-1} (C=CH bending), 1450 cm^{-1} (C−CN wing stretching), 1600 cm^{-1} (C=C ring stretching), and ca. 2225 cm^{-1} (C−N stretching) (spectrum a), which correlate well with the literature.[51] For the CuTCNQ sample (spectrum b), it can be seen that the C−CN wing stretching vibration mode is shifted to 1380 cm^{-1}, and the C−N stretching band is shifted to 2200 cm^{-1} in comparison with TCNQ (spectrum a), both of which are indicative of $TCNQ^-$. Significantly, for CuTCNQ reacted with 1 mM $KAuBr_4$ (spectrum c), the presence of a C−CN wing stretching vibration mode at 1450 cm^{-1} illustrates the formation of neutral TCNQ (as seen in spectrum a) and a small shifted feature at 1380 cm^{-1} (as seen in spectrum b). The full Raman study involving reactions with an increasing concentration of gold salt is illustrated in the Supporting Information (Figure S4), which shows the gradual appearance of the C−CN wing stretching vibration mode at 1450 cm^{-1} associated with TCNQ, as the gold concentration is increased during the reaction. The 1450 cm^{-1} feature after reaction with gold salt can therefore be confidently associated with a reaction product and not a contaminant, as the pristine CuTCNQ sample (spectrum b) shows no evidence of this band. This also suggests that, under conditions employed in this study, most of the TCNQ that is formed during the reaction is not liberated into the solution as observed by UV−vis spectroscopic analysis (Figure 3).

To support the XPS results (Figure 2b) and to ensure that the formation of metallic gold was achieved during the reaction of CuTCNQ with $KAuBr_4$, XRD spectra of CuTCNQ reacted with the different gold salt concentrations was performed (Figure 5). The pristine TCNQ powder (pattern a) shows major peaks at 18.6°, 24.2°, 26.0°, 27.5°, 28.5°, and 30.1° 2θ that correspond to monoclinic TCNQ and agree well with the literature (JCPDS card 00-033-1899). The pristine CuTCNQ substrate (pattern b) shows two peaks at 16.0° and 18.0° 2θ that are attributable to phase I CuTCNQ

(50) Liu, S.-G.; Liu, Y.-Q.; Wu, P.-J.; Zhu, D.-B.; Tien, H.; Chen, K.-C. *Thin Solid Films* **1996**, *289*, 300–305.

(51) Kai, X.; Jing, T.; Zhengwei, P.; Alex, A. P.; Ilia, N. I.; Stephen, J. P.; David, B. G. *Angew. Chem., Int. Ed.* **2007**, *46*, 2650–2654.

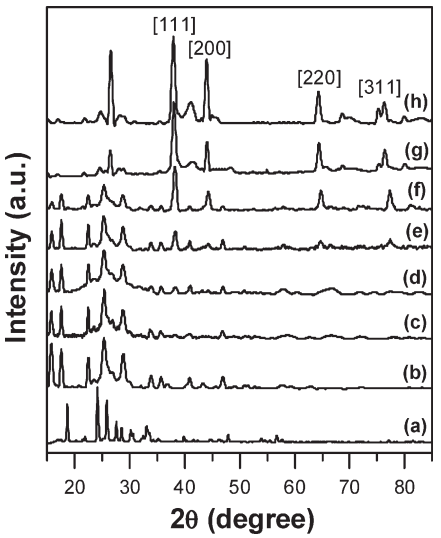

Figure 5. XRD patterns of (a) pristine TCNQ crystals, (b) pristine CuTCNQ microrods, and (c−h) CuTCNQ reacted with (c) 1 μM, (d) 10 μM, (e) 50 μM, (f) 100 μM, (g) 500 μM, and (h) 1 mM $KAuBr_4$. Peaks corresponding to fcc gold planes have been labeled.

(00-054-1997). In addition to these two peaks, a collection of three peaks at 22.5°, 25.0°, and 29.0° 2θ can also be attributed to CuTCNQ and correspond well with the literature.[1] When 1 μM $KAuBr_4$ is introduced (pattern c), little change is observed in both the intensity and position of peaks, which corresponds well with the SEM image shown in Figure 1c that describes no significant decoration with gold particles. As the concentration of $KAuBr_4$ is increased to 10 μM (pattern d), peaks attributed to CuTCNQ at 16.0°, 18.0°, 22.5°, 25.0°, and 29.0° 2θ are observed to reduce in intensity. This is consistent with the SEM images shown in Figure 1d typifying the dissolution of CuTCNQ into the reaction medium. Also of note is the appearance of a small peak attributable to the [111] plane of face-centered cubic (fcc) gold at 38° 2θ (03-065-2870). A further increase of the $KAuBr_4$ concentration to 50 μM (pattern e) results in a greater reduction in intensity of the peaks associated with CuTCNQ, along with concomitant increase in the Au [111] peak at 38.0° with additional fcc Au peaks at 44.5°, 65.0°, and 78.0° 2θ corresponding to the [200], [220], and [311] crystal planes, respectively. The addition of 100 μM $KAuBr_4$ (pattern f) results in a further reduction in intensity of the CuTCNQ peaks and an increase in the peaks associated with metallic gold. Upon the addition of 500 μM $KAuBr_4$ (pattern g), an almost complete reduction in intensity of the CuTCNQ peaks with a simultaneous increase in the intensity of the fcc gold peaks is observed. Finally, the addition of 1 mM $KAuBr_4$ (pattern h) results in the increased intensity of a peak at 27.5° 2θ, which could be attributed to a combination of both CuTCNQ and TCNQ peaks and an increase in those attributed to fcc gold, which again correlates well with the SEM image (Figure 1h).

4. Mechanism of Galvanic Replacement

The SEM, EDX, UV−visible, Raman, FT-IR spectroscopy, and XRD analyses demonstrate a stark difference in the morphology and composition of both the reactant solution and the CuTCNQ substrate as the concentration of $KAuBr_4$ is increased during the galvanic replacement reaction, suggesting a combination of two reaction mechanisms. In the absence of $KAuBr_4$, the CuTCNQ rods are observed to dissolve in acetonitrile solvent to form hollow CuTCNQ rods, indicating the dissolution of phase I CuTCNQ into the solvent as described by eq 1:

$$CuTCNQ_{(s)} \rightarrow Cu^{+} + TCNQ^{-} \quad (1)$$

Conversely, when $KAuBr_4$ is introduced into acetonitrile, the dissolution of CuTCNQ into the solvent is found to reduce (signatures of $TCNQ^{-}$ ions are reduced) and the amount of $TCNQ^{0}$ formed in the solvent increases (UV−vis spectroscopy, Figure 3). This suggests that a redox reaction that is akin to a galvanic replacement process occurs between CuTCNQ and $KAuBr_4$ and results in the decoration of phase I CuTCNQ with Au particles, which can be described by eq 2:

$$3CuTCNQ + KAuBr_4 \rightarrow Au^{0} + 3TCNQ^{0} + 3CuBr + KBr \quad (2)$$

It has been demonstrated by Bond et al.[46] that CuTCNQ oxidizes over a potential range of 0.500 to 0.700 V (vs SHE), whereas the standard reduction potential for the $AuBr_4^{-}$/Au couple is 0.854 V (vs SHE),[52] which provides enough driving force for this reaction to be thermodynamically possible. The possibility of $AuBr_4^{-}$ ions reacting with Cu^{+} ions to form Au^{0} can be discounted, as Cu^{+} ions are highly stable in acetonitrile and not readily oxidized where the standard potential for the Cu^{2+}/Cu^{+} couple has been reported to be 1.291 V (vs SHE).[46] Notably, this is the first time, to the best of our knowledge, that the galvanic replacement of a semiconducting charge transfer complex has been reported. At higher concentrations of $KAuBr_4$ (> 100 μM), it seems that the galvanic replacement reaction is the dominant process, which results in little CuTCNQ dissolution but in the formation of neutral TCNQ that diffuses into the reactant solution. Indeed the replacement reaction becomes so dominant at the highest gold salt concentrations studied (1 mM) that neutral TCNQ is found in the CuTCNQ/Au composite (as seen by Raman and XRD analysis), suggesting that the reaction is extremely rapid, which instantaneously covers any TCNQ formed during the reaction with Au nanoparticles and prevents its dissolution.

To rule out the possibility of pinholes in the CuTCNQ film which might expose the underlying metallic copper film where galvanic replacement could occur, CuTCNQ crystals were removed from the surface of Cu foil and then directly reacted with $KAuBr_4$ in acetonitrile in the absence of Cu foil. In this case also, the isolated CuTCNQ microrods decorated with Au nanoparticles were observed (Supporting Information, Figure S5). The same general trend is observed in that CuTCNQ decoration with Au particles becomes more significant at higher gold salt concentrations, with interestingly hollow cubic-shaped particles being formed at a higher $KAuBr_4$ concentration of 1 mM. The appearance of hollow Au cubes during galvanic replacement of a semiconductor CuTCNQ by metal ions is interesting and corroborates well with previous galvanic replacement studies involving a metal/metal ion couple.[41] Interestingly, when the $KAuBr_4$ concentration was further increased to 10 mM, a significant

(52) Evans, D. H.; Lingane, J. J. *J. Electroanal. Chem.* **1963**, *6*, 1–10.

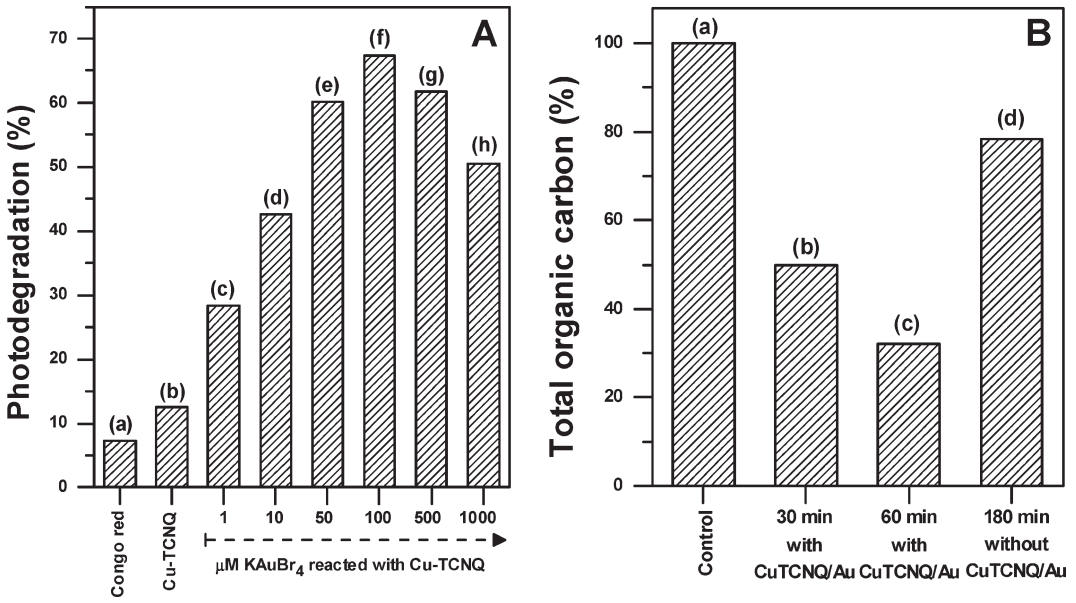

Figure 6. (A) Percentage photodegradation of 50 μM aqueous solution of the organic dye Congo red under simulated solar light conditions for 30 min as recorded by UV−vis spectroscopy: (a) Congo red, (b) pristine CuTCNQ, and (c−h) CuTCNQ reacted with (c) 1 μM, (d) 10 μM, (e) 50 μM, (f) 100 μM, (g) 500 μM, and (h) 1 mM $KAuBr_4$. (B) Percentage total organic carbon obtained from Congo red (a) before and (b−d) after its exposure to simulated solar light for (b) 30 min and (c) 60 min in the presence of the CuTCNQ/Au nanocomposite and (d) 180 min in the absence of the CuTCNQ/Au nanocomposite.

increase in the decoration of CuTCNQ with Au cubes was observed. The formation of such structures on the CuTCNQ surface once again reaffirms the possibility of performing galvanic replacement reactions on semiconducting surfaces.

The decoration of semiconducting materials such as TiO_2 with metal nanoparticles to improve their photocatalytic properties through better interfacial charge transport and charge separation under band gap excitation conditions is well established.[53−56] Since the phase I CuTCNQ/Au microrods synthesized in this study have not hitherto been reported, the possibility of using such materials for the photocatalytic degradation of "Congo red", an organic dye, was explored in the presence of simulated solar radiation. The molecular structures of phase I CuTCNQ and Congo red are depicted in the Supporting Information (Figure S6). Shown in Figure 6A are the photodegradation percentages of the phase I CuTCNQ substrates galvanically replaced with differing amounts of $KAuBr_4$ after irradiation by solar light for 30 min when compared with a stock solution containing 50 μM Congo red dye by taking the absorbance (A_{max}) intensity of Congo red at 500 nm into account. When no CuTCNQ substrate is present (a), the solar radiation causes degradation of ca. 7% of the dye, which increases to ca. 12% upon the introduction of an unmodified CuTCNQ substrate (b), indicating that phase I CuTCNQ has a degree of photocatalytic activity. When the CuTCNQ substrate is galvanically replaced with 1 μM $KAuBr_4$ (c), the dye degradation increases to ca. 28%. With increasing concentrations of $KAuBr_4$, the photodegradation of dye molecules is found to increase to ca. 42% (d, 10 μM $KAuBr_4$), ca. 60% (e, 50 μM $KAuBr_4$), and to a maximum of ca. 67% (f, 100 μM $KAuBr_4$) within 30 min of reaction. However, further increasing the $KAuBr_4$ concentration to 500 μM and 1 mM $KAuBr_4$ (g and h, respectively) leads to a decrease in the photocatalytic activity of the CuTCNQ/Au substrate to ca. 61% and ca. 51%, respectively, within 30 min of reaction. It is well-known that the extent of metal loading on the surface of a photocatalyst is correlated to the efficiency of the material, and that above the optimum metal content the efficiency is observed to decrease.[57] As such, great care must be taken to ensure that a quantity of metal that provides optimum photocatalytic activity is used for improved photocatalytic performance. Although UV−vis spectroscopy experiments revealed significant degradation of Congo red in the presence of CuTCNQ/Au nanocomposites, it is likely that the degradation products of organic dyes might still be present in the solution in the form of colorless organic products. Therefore, additional measurements were performed wherein total organic carbon (TOC) contents of Congo red containing solutions were determined in a time-dependent fashion after their exposure to one of the CuTCNQ/Au nanocomposites (sample obtained using 1 mM $KAuBr_4$). The TOC measurements shown in Figure 6B clearly indicate a more than 50% reduction in the TOC content of the solution after 30 min of exposure to the CuTCNQ/Au composite (Figure 6Bb), which further reduces by 68% after 60 min (Figure 6Bc). In comparison, only a 21% reduction in TOC content was observed when Congo red was exposed to simulated solar radiation for 3 h in the absence of the CuTCNQ/Au nanocomposite (Figure 6Bd). This can be considered as highly significant photocatalytic performance for a novel CuTCNQ/Au material, which has not hitherto been reported for its photocatalytic properties. It is also noteworthy that although traditional metal-decorated metal oxides such as TiO_2 might achieve better photocatalytic performance than that demonstrated by the CuTCNQ/Au system in our study, the

(53) Dawson, A.; Kamat, P. V. *J. Phys. Chem. B* **2001**, *105*, 960–966.
(54) Du, L.; Furube, A.; Yamamoto, K.; Hara, K.; Katoh, R.; Tachiya, M. *J. Phys. Chem. C* **2009**, *113*, 6454–6462.
(55) Jakob, M.; Levanon, H.; Kamat, P. V. *Nano Lett.* **2003**, *3*, 353–358.
(56) Hidalgo, M. C.; Navío, J. A.; Colón, G *J. Phys. Chem. C* **2009**, *113*, 12840–12847.
(57) Linsebigler, A. L.; Lu, G.; Yates, J. T; Maicu, M.; Navío, J. A. *Chem. Rev.* **1995**, *95*, 735–758.

demonstration that semiconductor CuTCNQ/Au composites are able to show solar light photocatalytic performance is highly significant, with a scope for further development, particularly for visible light photocatalysis.

5. Conclusions

In this work, we have demonstrated that microrods of phase I CuTCNQ can be decorated with metallic Au from an acetonitrile solution containing $KAuBr_4$ by a galvanic replacement mechanism. Under conditions of low gold salt concentration, the dissolution of CuTCNQ occurs and results in the formation of hollow rods. This dissolution process becomes more inhibited as the redox reaction between phase I CuTCNQ and Au^{3+} ions takes effect, which results in extensive coverage of CuTCNQ with metallic Au, with evidence of surface confined neutral TCNQ formation that is inaccessible to the acetonitrile solution. Interestingly, the phase I CuTCNQ/Au composite materials showed promising photocatalytic properties for the destruction of organic dyes such as Congo red, whose performance was found to be dependent on the surface coverage of CuTCNQ with Au particles. This approach opens up the possibility of studying other metal−TCNQ semiconductor complexes that could be replaced with noble metals such as gold, platinum, and palladium and may have interesting applications particularly in catalysis and sensing.

Acknowledgment. V.B. thanks the Australian Research Council (ARC) for APD Fellowship and financial support through the ARC Discovery Project DP0988099 and acknowledges the support of Ian Potter Foundation in establishing a multimode advanced spectroscopy facility at RMIT University. A.P.O. thanks the Platform Technologies Research Institute for financial support. V.B., A. P.O., and S.K.B. thank the ARC for financial support through Linkage Project LP100200859 and Discovery Project DP110105125.

Supporting Information Available: Additional SEM images; detailed EDX, FT-IR, and Raman analysis of CuTCNQ samples galvanically replaced with different concentrations of $KAuBr_4$; and molecular structures of phase I CuTCNQ and Congo red. This material is available free of charge via the Internet at http://pubs.acs.org.